SEISMIC PERFORMANCE OF PRESTRESSED CONCRETE MASONRY WALLS INCORPORATING ENERGY DISSIPATORS

P. T. Laursen[1]

[1] *Asst. Professor, Dept. of Architectural Engineering , California Polytechnic State University,*
San Luis Obispo, California, USA
Email: plaursen@calpoly.edu

ABSTRACT:

This paper explores the seismic in-plane response of post-tensioned fully grouted concrete masonry (PCM) walls with and without energy dissipating devices. A typical 3-story PCM structure was subjected to ground motions representative of the seismic hazard in the Los Angeles, California. The viability of PCM walls as the lateral system was evaluated and the efficiency of incorporating energy dissipators in the wall-base interface was investigated.

KEYWORDS: Masonry, Prestressing, Shear wall, Seismic performance, Energy dissipation,

1. INTRODUCTION

This paper explores the seismic in-plane response of post-tensioned fully grouted concrete masonry (PCM) walls with and without energy dissipating devices incorporated. Laursen (2001) found that only a limited amount of hysteretic energy is dissipated during large displacement cycling of PCM walls. Experiments by Laursen (2004) showed that hysteretic energy dissipation can be increased significantly by incorporating energy dissipators in the wall/foundation interface.

Lateral displacement response is critical to the PCM wall performance due to limited energy dissipation. The specific objective of this paper is to explore the effect of the presence of simple energy dissipators on the structural response. Inelastic numerical analysis is used to determine the wall lateral displacement demand for a series of walls with and without energy dissipators.

The question is if these energy dissipators are efficient for
- increasing the wall strength
- reducing the wall displacements
- reducing the scatter in displacement response to the suite of ground motion

2. BACKGROUND

Using unbonded post-tensioning, walls are vertically prestressed by means of strands or bars which are passed through vertical ducts inside the walls. As the walls are subjected to lateral displacements, gaps form at the horizontal joints, reducing the system stiffness. As long as the prestressing strands are kept within the elastic limit, or at least maintain a considerable amount of the initial prestressing force, they can provide a restoring force, which will return the walls to their original alignment upon unloading. The wall moment-displacement response can be characterized as bi-linear elastic when no energy dissipators are incorporated, see Figure 1(a). When energy dissipators based on yielding of steel are incorporated in the horizontal wall joint at the base, the moment-displacement response is flag-shaped, see Figure 1(b).

An extensive testing program on PCM walls was conducted at the University of Auckland (Laursen 2001, 2004a, 2004b). It was found that rocking behavior was characteristic for the wall response to in-plane simulated seismic loading. It was also found that the wall displacement capacity before excessive loss of lateral strength was governed by the degree of confinement provided in the plastic deformation zones (wall toes), see Figure 1.

(a) No energy dissipators   (b) With energy dissipators

Figure 1-PCM wall behavior   Figure 2-Energy dissipation bar
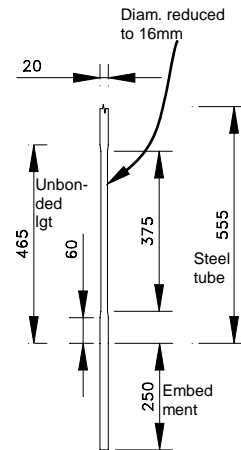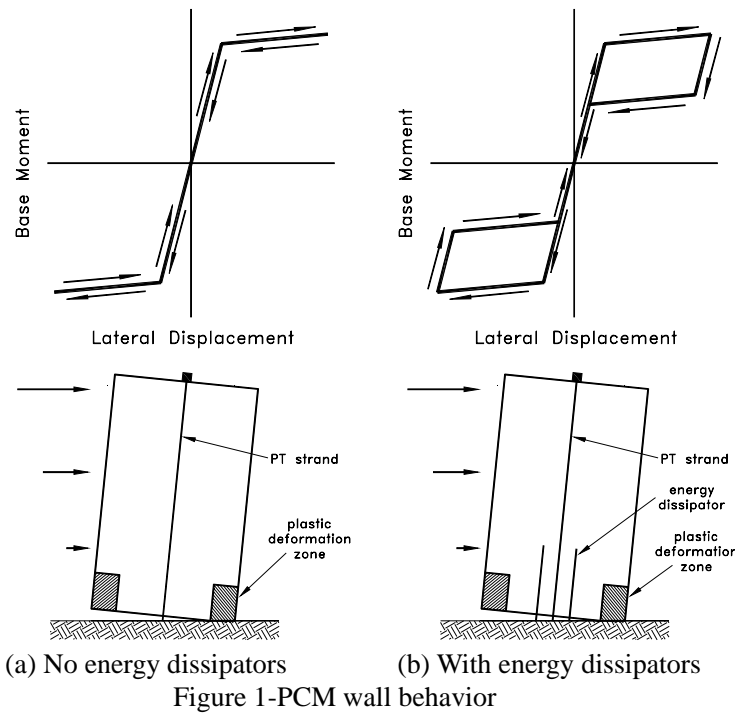
Walls constructed with ½-height masonry units (90 mm high) and confining plates in each bed joint in the plastic deformation zone showed the highest displacement capacities. Use of ½-height masonry units allows placing of twice as many confinement plates and superior confinement of the masonry.

Two structural tests by Laursen (2004a) are of particular interest to this study: FG:L3.0-W15-P2-CP-CA (referred to as CA) and FG:L3.0-W15-P2-CP-CA-ED (referred to as CA-ED). The wall panels were identical, except for that CA-ED had energy dissipators incorporated in the wall-base interface. The grouted walls were 3.0 m long, 2.6m tall and constructed of 0.14 m thick concrete masonry units. Both walls had two prestressing bars providing axial force and bed joint confinement plates embedded in the lower corners. Figure 2 shows the geometry of one of the two 'dog-bone'-type energy dissipators embedded in CA-ED. The milled part of the bars was designed such that the axial prestressing force comfortably could yield the bars in compression, thus forcing the wall back to its original alignment upon unloading. An energy dissipator yield force to prestressing force ratio of approximately 1:3 was chosen for this test. The bar was confined by heavy steel tube to ensure that the section of bar intended to yield would not buckle when forced into compression. Further details on the tests can be found in Laursen (2004a).

The lateral force-displacement response of the walls is shown in Figure 3 (only one quadrant depicted). The 'pinched' loops shown in Figure 3(a) indicate that the CA wall behaved in an essentially non-linear elastic fashion and did not dissipate much energy during cycling. The 'fat' loops shown in Figure 3(b) resemble the 'flag'-type of behavior shown in Figure 1(b) and indicate that the CA-ED wall did dissipate a significant amount of energy during cycling.

Parallel testing of reinforced concrete panels incorporating energy dissipators was conducted by Restrepo (2007).

3. PROTOTYPE WALLS

PCM walls are likely to be used for low rise structures, such as office buildings. The selected prototype structure is a 3-story building located in the Los Angeles, CA area.

(a) CP-CA

(b) CP-CA-ED
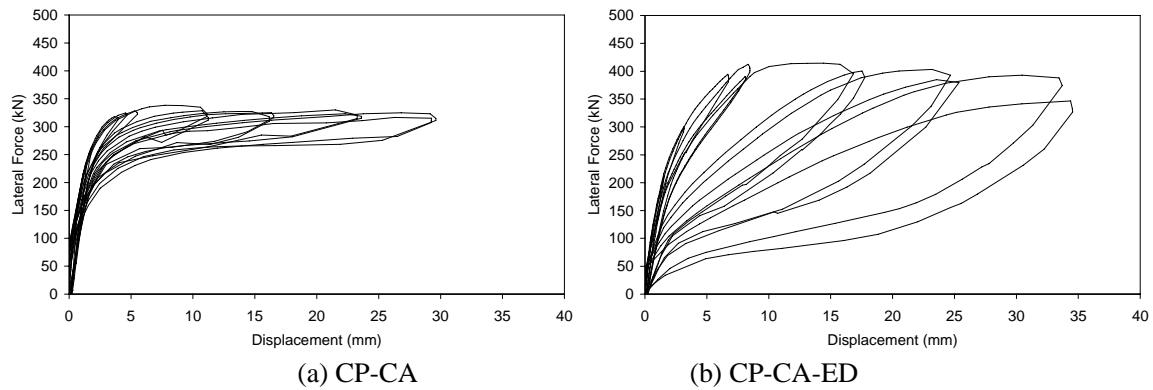
Figure 3-Force-displacement response
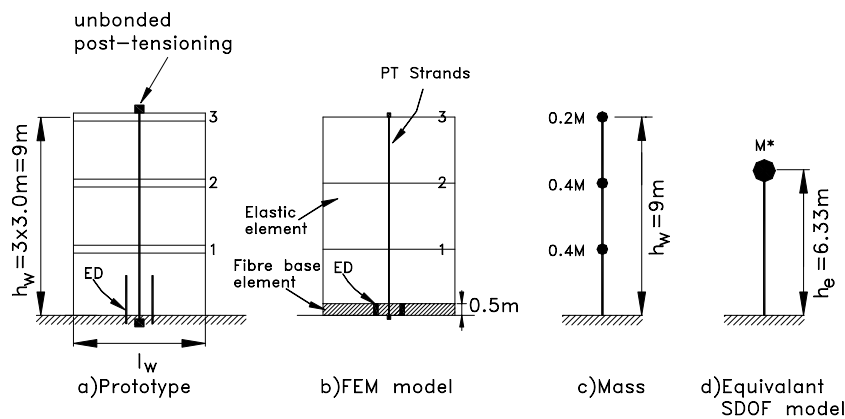
Figure 4-Prototype wall and modeling

Figure 4 shows the prototype walls schematically. The wall length l_w is 5.0m or 6.0m and height h_w is 9.0m. The story height is 3.0m and the wall thickness t_w is 0.19m. Table 1 shows seismic weight, the geometry and reinforcement of all walls analyzed. The period of vibration for walls L6 and L5 based on gross sectional properties are 0.15s and 0.18s, respectively.

In Table 3, L refers to wall length, EL refers to a linear elastic calculation with a wall of unlimited strength, P is number of prestressing strands, E refers to the ratio of yield force of the energy dissipators to the sum of axial forces due to prestressing, dead load and live load $r_{ED} = F_{yed}/(F_{pse}+P_u)$. E.g. L6-P6-E0.18 means a wall of 6.0m length with 6 prestressing strands and an energy dissipator embedded with a strength of 18% of $F_{pse}+P_u$. The number n_{pt} represents the total number of prestressing strands, f_{se} and F_{pse} the stress and force, respectively, in the cables at zero lateral displacement, F_{yed} the total yield force of all dissipator bars, P_u the factored axial load on the wall, $\xi = (F_{pse}+P_u)/(L_w b_w f'_m)$ is the axial load ratio in the wall and W_s is the total seismic weight carried by the wall. Parameters pertaining to wall strength requirements (n_{pt}, f_{se}, F_{pse}, F_{yed}) are discussed below. P_u and W_s were based on a realistic structural configuration.

Material properties for the prototype walls are given in Table 2, where f'_m and f'_{mc} are the concrete masonry strengths for regular (unconfined) and confined grouted concrete masonry, respectively, ε_{mu} is the extreme fiber strain for regular masonry at nominal flexural strength, ε_{muc} is the extreme fiber strain for confined concrete masonry at ultimate displacement capacity, E_m is the masonry Young's modulus, f_{py} and f_{pu} are the yield and rupture strengths of the prestressing strand (140mm^2 super strand), E_{ps} is the prestressing steel Young's modulus, f_y and E_s are the yield strength and Young's modulus of the energy dissipators. The strain capacity ε_{muc} is based on use of ½-height masonry units and bed joint confinement in the plastic deformation zone.

Table 1-Prototype wall geometry

Wall	n_{pt}	f_{se}	F_{pse}	F_{yed}	P_u	r_{ED}	ξ	W_s
L6-EL	-	-	-	-	-	-	-	2123
L6-P8	8	60%	1062	-	611	-	0.092	2123
L6-P6	6	60%	797	-	611	-	0.077	2123
L6-P6-E0.18	6	60%	797	260	611	0.18	0.091	2123
L6-P6-E0.33	6	60%	797	470	611	0.33	0.103	2123
L6-P4-E0.50	4	60%	531	571	611	0.50	0.094	2123
L5-EL	-	-	-	-	-	-	-	2055
L5-P10	10	67%	1483	-	570	-	0.135	2055
L5-P10-E0.24	10	67%	1483	492	570	0.24	0.167	2055
L5-P10-E0.33	10	67%	1483	687	570	0.33	0.180	2055
L5-P8	8	67%	1186	-	570	-	0.116	2055
L5-P8-E0.23	8	67%	1186	406	570	0.23	0.142	2055
L5-P8-E0.33	8	67%	1186	585	570	0.33	0.154	2055
L5-P8-E0.50	8	67%	1186	876	570	0.50	0.173	2055
	-	%fpy	kN	kN	kN	-	kN	kN

Table 2-Prototype wall material properties

f'_m	16 MPa
f'_{mc}	18 MPa
ε_{mu}	0.0025
ε_{muc}	0.0130
E_m	14400 MPa
f_{py}	1561 MPa
f_{pu}	1860 MPa
E_{ps}	190000 MPa
f_y	414 MPa
E_s	200000 MPa

4. GROUND MOTIONS AND RESPONSE STATICS

Two sets of 20 ground motions were developed in conjunction with the SAC study for the Los Angeles region representing probabilities of exceedance of 2% and 10% in 50 years (return periods of 2475 and 475 years)(Somerville et al. 1997). The 10% in 50 years records were used for the present analysis. The ground motions were developed for analysis of 3-, 9-, and 20-story buildings and therefore appropriate for this study of 3-story masonry buildings.

The dynamic response of each wall to each of the 20 ground motions was determined by non-linear time-history analysis. The peak value of the structural response or demand, x_i, for each ground motion was recorded. Median values $\hat{x}$, defined as the geometric mean, and the dispersion measure, δ, of n (=20) observed values of x_i of the response were calculated. Assuming the response is Log-normal distributed, the 84th percentile (16% probability of exceedance) can be calculated as x_{84} (Benjamin (1970)).

$$\hat{x} = \exp\left[\frac{\sum_{i=1}^n \ln x_i}{n}\right] \quad ; \quad \delta = \sqrt{\frac{\sum_{i=1}^n (\ln x_i - \ln \hat{x})^2}{n-1}} \quad ; \quad x_{84} = \hat{x}\exp(\delta) \tag{4.1}$$

5. SIMPLE PREDICTION MODEL

Analytical prediction of the back-bone curve for Wall L6-P8 is shown in Figure 5 and follows the procedure reported in Laursen (1999) and Laursen (2002). This model enables estimation of wall base moment and lateral displacement at the wall equivalent height, h_e, for 4 limit states as shown in Figure 5.

Calculation of the nominal strength is modified to account for the presence of energy dissipator bars as follows:

$$M_n = \left(F_{pse} + \Delta F_{ps} + F_{yed} + P_u\right)\left(\frac{l_w}{2} - \frac{a}{2}\right) \quad \text{where} \quad a = \frac{F_{pse} + \Delta F_{ps} + F_{yed} + P}{\alpha f'_m t_w} \tag{5.1}$$

In Eqn. 5.1 ΔF_{ps} represents the tendon force increase due to deformation at the nominal strength limit state, and f'_m is taken as f'_{mc} and α = 0.94 for confined masonry. Table 3 shows wall nominal flexural strength predictions ϕM_n for all prototype walls assuming ϕ = 0.8 as specified in ACI 530-08/ASCE 5-08/TMS 402-08 for prestressed masonry. A reference estimate for the inelastic moment demand at the base of the walls is based on an estimated S_{DS} of 1.2g and ASCE 7-05 which allows R = 5 for special reinforced masonry shear walls and R = 1.5 for prestressed masonry shear walls. In this paper the reference response modification factor R is taken as 4 based on expectation of ductile response, resulting in an inelastic moment demand M_u at the base of approximately 4,000 kNm.
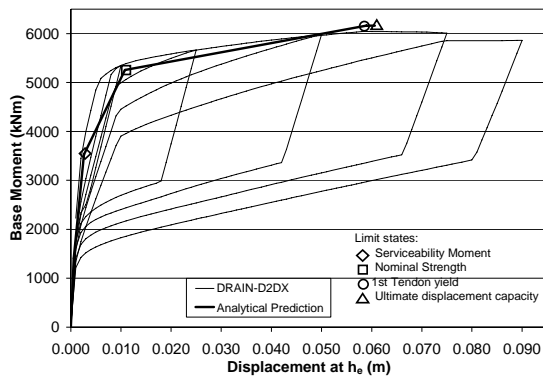
Figure 5-L6-P6-E0.33, Analytical prediction and Fiber model
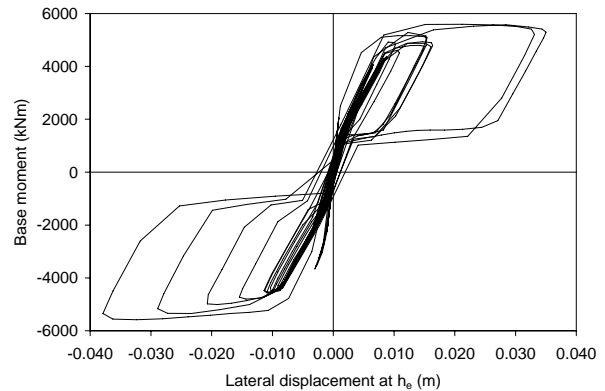
Figure 6-Wall L6-P4-E0.50 dynamic response to Ground motion 02

The required prestressing force is determined such that $M_u \leq \phi M_n$ The required number of prestressing strands is determined based on a maximum allowed stress in the prestressing strands such that first yield of any prestressing strands coincides with the maximum allowed drift ratio. The ratio of energy dissipator yield force to wall axial force due to prestressing, live load and dead load, r_{ED}, was varied between 0.18 and 0.50 in order to explore various levels of damping, yet keeping the dissipator yield force sufficiently low to allow the combination of permanent axial force and the prestress force to comfortably force the wall back to it's original alignment.

Wall displacement capacity is a central issue for PCM walls. Although confinement as described in this paper enhances the wall displacement capacity by increasing the strain capacity of plain grouted concrete masonry, it is challenging to achieve as high a degree of confinement that is readily achievable for reinforced concrete. Despite using sophisticated finite element modeling to capture PCM wall behavior, it is difficult for these models to capture strength degradation. This underlines the need for a method for estimating the wall displacement capacity, d_u, based on empirical data. Large scale testing of PCM walls by Laursen (2004b) using confined ½-height concrete masonry suggested that the ultimate displacement capacity can be based on a masonry strain of $\varepsilon_{muc} = 0.013$ (Table 2) and a plastic deformation zone height of $h_p = 0.076h_e$. The ultimate displacement capacity, d_u, and drift ratio, Δ_u, with respect to the effective height, h_e, are assessed by Eqn. 5.2. Where ε_{mu} is taken as ε_{muc} and $\beta = 0.96$ for confined masonry.

$$d_u = \frac{h_p \left(h_e - \frac{h_p}{2} \right)}{c} \varepsilon_{mu} \quad \text{where} \quad c = \frac{a}{\beta} \quad \text{and} \quad \Delta_u = \frac{d_u}{h_e} \tag{5.2}$$

6. FIBER ELEMENT MODELING

DRAIN-2DX (Prakash (1993)) finite element models of all walls were created using a fiber beam-column element to model the rocking interface between the wall and foundation, beam elements to model the remainder of the wall panel and nonlinear truss elements to model the prestressing cables. The fiber element vertically extended 0.5m (=h_p). Similar models were validated by Laursen (2002) and Perez (2007). The stress-strain relationship for confined concrete masonry was based on the modified Elder-Priestley model developed by Laursen (2002).

Figure 5 compares the fiber element model static cyclic loading response for wall L6-P6-E0.33 with the simple predictions discussed in Section 5 and reveals excellent agreement. It is observed that the fiber models are not able to capture strength degradation and ultimate displacement capacity.

Table 3-Predictions and response quantities

Wall	M_n	ϕM_n	d_u	Δ_u	M_b $\hat{x}$	δ	x_{84}	d_e $\hat{x}$	δ	x_{84}	Δ_e $\hat{x}$	x_{84}	R_n $\hat{x}$	δ	x_{84}	R	C_d $\hat{x}$	δ	x_{84}
L6-EL	-	-	-	-	13937	0.52	23397	6.3	0.52	11	-	-	-	-	-	-	-	-	-
L6-P8	4786	3829	67	1.06	5526	0.12	6229	25	0.99	66	0.39	1.04	2.5	0.45	3.9	3.6	3.9	0.80	8.7
L6-P6	4088	3270	80	1.27	4928	0.13	5637	31	1.07	90	0.48	1.42	2.8	0.45	4.4	4.3	4.9	0.91	12.1
L6-P6-E0.18	4743	3794	68	1.08	5378	0.12	6049	25	0.99	66	0.39	1.04	2.6	0.45	4.1	3.7	3.9	0.80	8.7
L6-P6-E0.33	5256	4205	61	0.97	5753	0.12	6480	21	0.96	55	0.33	0.87	2.4	0.45	3.8	3.3	3.3	0.76	7.2
L6-P4-E0.50	4823	3858	67	1.06	5398	0.10	5964	25	0.88	61	0.40	0.96	2.6	0.47	4.1	3.6	4.0	0.75	8.4
L5-EL	-	-	-	-	14079	0.60	25519	9.4	0.60	17	-	-	-	-	-	-	-	-	-
L5-P10	4620	3696	56	0.89	5215	0.06	5514	42	0.85	100	0.67	1.57	2.7	0.55	4.7	3.8	4.5	0.69	9.0
L5-P10-E0.24	5496	4397	45	0.71	5932	0.05	6234	35	0.77	75	0.55	1.19	2.4	0.57	4.2	3.2	3.7	0.63	6.9
L5-P10-E0.33	5823	4658	42	0.66	6209	0.05	6555	32	0.79	70	0.50	1.10	2.3	0.57	4.0	3.0	3.4	0.61	6.2
L5-P8	4053	3242	65	1.03	4705	0.07	5032	50	0.86	119	0.79	1.88	3.0	0.55	5.2	4.3	5.4	0.67	10.5
L5-P8-E0.23	4820	3856	53	0.84	5327	0.06	5661	39	0.83	89	0.62	1.41	2.6	0.56	4.6	3.7	4.2	0.63	7.9
L5-P8-E0.33	5143	4114	49	0.78	5575	0.06	5915	35	0.79	76	0.55	1.21	2.5	0.56	4.4	3.4	3.7	0.62	6.9
L5-P8-E0.50	5644	4515	44	0.70	6002	0.06	6395	31	0.78	68	0.49	1.07	2.3	0.56	4.1	3.1	3.3	0.61	6.1
	kNm	kNm	mm	%	kNm	-	kNm	mm	-	mm	%	%	-	-	-	-	-	-	-

Table 3 shows the results of running the 20 ground motions for each wall. M_b is the base moment, d_e is the lateral displacement at h_e, Δ_e is the corresponding drift demand, R_n is the response modification coefficient based on the ratio M_b(elastic)/M_b(in-elastic). R is the response modification factor defined as M_b($\hat{x}$, EL model)/ϕM_b. C_d is the amplification of displacement response with respect to the purely elastic response (EL). Figure 6 shows wall L6-P4-E0.50 response to ground motion 02 and demonstrates the flag-shaped response.

8. DISCUSSION

Efficient wall design should be based on a R-factor as high as possible while limiting the drift demand Δ_e to the lesser of the drift capacity Δ_u and the allowable drift Δ_a. Such design approach may be termed displacement based design, where the structure is designed to reach a particular maximum displacement as a result of ground motion pertaining to the relevant limit state.

ASCE 7-05 limits Δ_a to 1% for masonry wall structures. When design is based on inelastic time-history analysis with more than 10 ground motions the drift demand Δ_e may be characterized by the mean (central value) response and is limited to $1.25\Delta_a = 1.25\%$. While $\Delta_e > 1.25\%$ is in violation with the code, it does not necessarily mean that the structure will sustain severe damage or fail. It merely implies that the lateral force system, other structural members and non-structural elements may sustain more damage than expected.

On the other hand, if the drift demand, Δ_e, surpasses the dependable drift capacity, Δ_u, the lateral force resisting system may fail. It is therefore of considerable interest to look at the dispersion of drift demand, δ, from the 20 ground motions when the wall drift capacity is the limiting factor for design.

8.1. Elastic response
Looking at the responses of the elastic walls models L6-EL and L5-EL with unlimited strength, is seen that a median base moment of approximately 14,000kNm develops for both walls and that there is 14% probability of the base moment exceeding approx 25,000kN.

8.2. Median response
The discussion in this section is based on the median response that may be interpreted as the expected wall response.

The median drift demands shown in Table 3 are permissible for all walls. Drift demands were significantly higher for L5 walls than L6 walls for a given flexural strength due to higher flexibility. Reference walls L6-P8 and L5-P10 are designed to achieve $\phi M_n = 4000$kNm. The drift demands are 0.39% and 0.67%, both lower than

the drift capacity and the allowable drift. R-factors of 3.6 and 3.8 were achieved. The displacement amplification factor C_d ranged between 3.3 and 4.9, values close to the value of 3.5 specified for special reinforced shear walls by ASCE 7-05.

Table 3 reveals that reducing the number of PT cables to 6 (L6-P6) and 8 (L5-P8) decreases the wall flexural strength and increases the drift demand and the R-factor. The drift demands are 0.48% and 0.79% for walls L6-P6 and L5-P8 respectively, and remain lower than the drift capacity and the allowable drift.

The succession of walls L6-P6/L6-P6-E0.18/L6-P6-E0.33, L5-P10/L6-P10-E0.24/L5-P10-E0.33 and L5-P8/L6-P8-E0.23/L5-P8-E0.33/L5-P8-E0.50 show that incorporation of energy dissipator bars increases the wall flexural strength, and decreases the drift capacity, the drift demand and the R-factor.

Wall L6-P4-E0.50 featured 4 PT cables and a relatively high energy dissipator strength, and achieved a flexural strength comparable to the strengths of L6-P8 and L6-P6-E0.18. Comparison of these walls (Table 3) indicates that the median displacement response of these three walls virtually are identical (response to the individual ground motions varied some). Contrary to expectation, the energy dissipator bars merely reduced the displacement response by increasing the flexural strength. Similar conclusions can be made comparing walls L5-P10 and L5-P8-E0.23 or comparing walls L5-P10-E0.33 and L5-P8-E0.50.

Failure of the energy dissipators to reduce displacement demand further than that caused by the flexural strength increase, can be attributed to: (1) hysteric damping is most efficient for damping of resonant motion which is contrasted by the nature of the ground motion suite that includes a significant number of motions with few and strong pulses (near fault characteristic), (2) the fact that wall periods of vibration are in the short period range (expectation of low displacement demand), (3) and to some extent that the amount of energy dissipated by the bars was too small to really affect the wall displacement response.

8.3. 84th percentile response

In the following discussion the 84th percentile response (=16% probability of exceedance) is considered a reasonable and 'safe' upper bound for the wall displacement demand, thus $\Delta_{e,x84} \le Min(\Delta_u, 1.25\%)$ is acceptable.

The 84th percentile (x_{84}) drift demands for all L6 walls, except L6-P6, indicate that these walls possess sufficient displacement capacity. L6-P6 drift demand $\Delta_{e,x84}$ exceeds both Δ_u, and $1.25\Delta_a$ by a margin of 12%. Conversely, the 84th percentile (x_{84}) drift demands for all L5 walls exceed Δ_u and in some cases also $1.25\Delta_a$. Using the 84th percentile (x_{84}) drift demands as the upper bound demand, all L5 walls designs are deemed un-safe.

Better confinement of the masonry in the plastic deformation zone will increase the masonry strain capacity, ε_{muc}, and consequently will increase the wall drift capacity, Δ_u (Eqn. 5.2), and will in some cases allow for use of the shorter L5 walls.

CONCLUSION

It is concluded that PCM walls likely can be used as a ductile lateral force resisting system for 3-story structures in high seismic areas.

A large amount of scatter (high δ) was found for the displacement response of PCM walls with or without energy dissipators. In order to mitigate this uncertainty, it was suggested that the 84th percentile drift response could be considered a reasonable and 'safe' upper bound for the wall drift demand.

It was demonstrated that the addition of energy dissipators in the wall-base interface did increase the wall strength and reduced the drift demand. However, it was also shown that the reduction in drift demand largely was caused by the strength increase and not by the additional energy dissipation, even for the relatively highly

damped walls L6-P4-E0.50 and L5-P8-E0.50. Furthermore, the presence of energy dissipators did not significantly reduce the scatter of the wall response to the 20 ground motions in comparison to the un-damped walls.

L6 walls performed well. The shorter walls, L5, exhibited 84 percentile displacement demands in excess of the displacement capacity, and were deemed unsafe. Better confinement of the masonry for L5 walls would increase the wall displacement capacity and allow for use of these walls.

REFERENCES

ACI 530-08/ASCE 5-08/TMS 402-08, Building Code Requirements and Specifications for Masonry Structures, The Masonry Society, Boulder, CO, USA

ASCE 7-05, Minimum Design Loads for Buildings and Other Structures, American Society of Civil Engineers, Structural Engineering Institute, Reston VA, USA

Benjamin, J. R., and Cornell, C. A. (1970), Probability, Statistics, and Decision for Civil Engineers, McGraw-Hill, New York, 684 pp.

Laursen, P.T., and Ingham, J.M. (1999), In-plane Response of Post-tensioned Concrete Masonry, *Journal of the Structural Engineering Society of New Zealand*, **Vol. 12, No. 2, September 1999**, pp. 21-39.

Laursen, P. T., Ingham, J. M. (2001), Structural Testing of Single-Storey Post-Tensioned Concrete Masonry Walls, *Journal of the Masonry Society*, **ISSN 0741-1294, 19, 1**, 69-82.

Laursen, P.T. (2002), Seismic Analysis and Design of Post-tensioned Concrete Masonry Walls, PhD dissertation, March, Department of Civil and Environmental Engineering, University of Auckland, New Zealand.

Laursen, P. T., Ingham, J. M. (2004a), Structural Testing of Enhanced Post-Tensioned Concrete Masonry Walls, *ACI Structural Journal*, **ISSN 0889-3241/98, 101, 6, Nov-Dec**, 852-862.

Laursen, P. T., Ingham, J. M. (2004b), Structural Testing of Large-Scale Post-Tensioned Concrete Masonry Walls, *ASCE Journal of Structural Engineering*, **ISSN 0733-9445, 130, 10,** 1-9.

Perez, F. J., Sause, R., Pessiki, S. (2007), Analytical and Experimental Lateral Load Behavior of Unbonded Posttensioned Precast Concrete Walls, *ASCE Journal of Structural Engineering*, **ISSN 0733-9445/2007/11-**1531-1540.

Prakash, V., Powell, G. and Campbell, S. (1993), DRAIN-2DX Base Program, User Guide; Version 1.10, Report No. UCB/SEMM-93/17, Department Engineering, University of California, Berkeley, California, 1993

Restrepo, J. I., and Rahman, A. (2007), Seismic Performance of Self-Centering Structural Walls Incorporating Energy Dissipators, *ASCE Journal of Structural Engineering*, **ISSN 0733-9445/2007/11-**1560-1570.

Somerville, P., Smith, N., Punyamurthula, S., and Sun, J. (1997). Development of ground motion time histories for phase 2 of the FEMA/SAC steel project, SAC Background Document Report No. SAC/BD-9/04, SAC Joint Venture, 555 University Ave., Sacramento, CA.